FINITE VOLUME SQUEEZE FLOW IN HIGHLY COMPRESSIBLE POROUS ANNULAR DISCS

Petrică TURTOI[1], Mircea D. PASCOVICI[2]

This paper presents an original theoretical model for the axisymmetric squeeze flow of a Newtonian fluid imbibed in the central region of a highly compressible porous layer. The fluid flow is studied for three squeezing conditions: constant speed, constant force and given impulse. The experimental validation of the model is made for reticulated polyurethane foam imbibed in central region with glycerin and subjected to squeeze with constant speed. The applications of this innovative configuration can be in domains like automotive, sport equipment and ballistic protection.

Keywords: lubrication, squeeze, porous material, polyurethane foam.

1. Introduction

The resistance to flow of a fluid through a porous medium is generated by viscous friction. This effect underlies the damping effect that occurs during compression of a porous material which has been imbibed with a fluid. The forces generated by squeezing the porous material can be neglected compared with hydrodynamic forces generated by the fluid flow through pores.

Damping capacity for highly compressible porous layers (HCPL) imbibed with liquids has been investigated in theoretical and experimental studies [1-3]. The high potential of this mechanism for protection against mechanical shock has already been shown in [4-7]. Theoretical and experimental studies have considered squeeze process at constant speed, under constant force and by impact. There were analyzed both conformal (disc on plane [8] or cylinder on plane contact [5]) and nonconformal contacts (sphere on plane contact [3] or cylinder on cylinder contact [4]). Several studies have been made [9-11] to assess damping capacity of reticulated porous foam that have portion of material replaced with low-density foam imbibed with liquid. During compression the fluid migrate outwardly to the higher-density foam. To study the fluid flow through porous structure, Dowson [9] proposes a model with two flow regimes. The model was improved later by Vossen [11]. Both assumed that the porous structure buckle and collapse under compression forming a band of densified layers of cells. This band is assumed to appear in the center of the specimen and propagates symmetrically

[1] PhD Student, Military Equipment and Technologies Research Agency, , e-mail: pturtoi@acttm.ro;
[2] Prof., Dept. of Machine Elements and Tribology, University POLITEHNICA of Bucharest, Romania, e-mail: mircea@meca.omtr.pub.ro.

towards the compression plates as the specimen is further compressed [11, 12]. Elasto-plastic damping capacity of dry layers was also analyzed [10, 12, 13]. The experimental study of Pampolini [13] showed that during compression, two regions with different porosity are generated. However the experimental study was made on relatively high thickness materials and the proposed model is quite complex.

In this paper the squeeze process between two parallel flat discs is analyzed. The element of originality is that the fluid is found initially only in central reservoir; the surrounding annular porous ring is dry. Both the central reservoir and the annular disk are made from the same porous material.

Experimental analysis is also original. The constant speed squeeze tests were made with polyurethane foam imbibed with glycerin or silicone oil.

2. Analytical model

A finite volume of Newtonian fluid imbibed in a central reservoir is squeezed out radially through a dry porous ring.

The squeeze is produced by a flat, rigid and impermeable disc of radius R_e (fig. 1). The HCPL is placed on a perfectly flat, rigid and impermeable surface. The two surfaces remain parallel during approach.

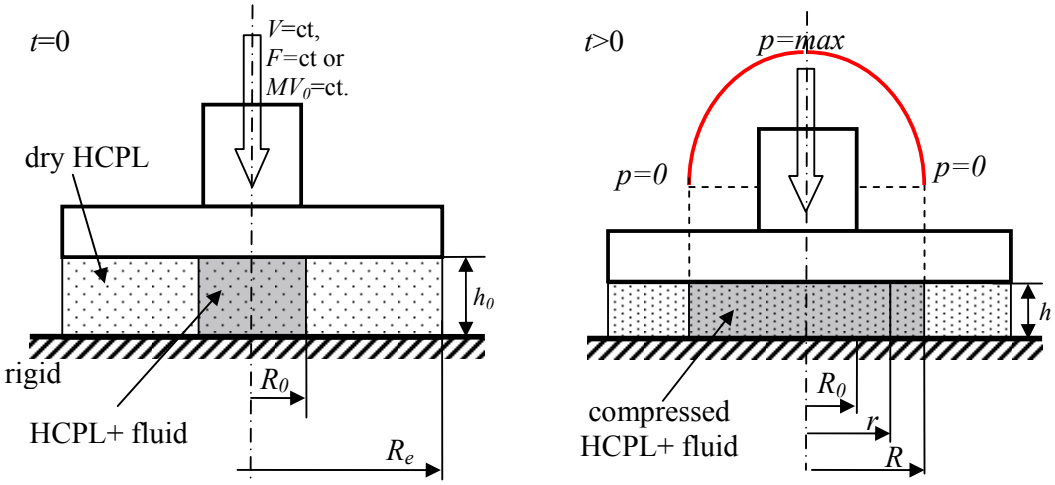

Fig. 1 Geometry of the model for porous material ring with fluid reservoir squeezed at constant speed

The central circular volume with radius R_0 and thickness h_0 is filled with fluid imbibed in the porous layer. Initially, the volume between R_0 and R_e with thickness h_0 is an annular dry layer. During squeeze process the fluid flows radially from the central reservoir through the dry porous material. The layer of

porous material imbibed at radius R and thickness h is subjected to squeeze. The theoretical model is axially symmetric (fig.1).

The following assumptions are made:

a. The fluid is Newtonian and the flow is laminar, isothermal and isoviscous;

b. The elastic forces generated by the solid structure of the porous material under squeeze can be neglected if compared with lift forces [1,16];

c. Fluid pressure is constant across HCPL thickness and the flow in radial direction can be described using Darcy law [2,3,15];

d. Because the HCPL is considered very thin and the cross-section does not change significantly, in normal squeeze, the product between thickness h and compactness σ can be considered constant: $\sigma h = \sigma_0 h_0 = \mathrm{ct}$;

e. Permeability is considered related with porosity ε, and correspondingly, to the compactness σ, using Kozeny-Carman equation [14];

$$\phi = D(1-\sigma)^3 / \sigma^2 \tag{1}$$

f. The pores of the material are assumed to be completely filled with fluid;

g. All the pores of the material are interconnected.

h. The conservation of the squeezed finite volume gives:

$$\pi R_0^2 h_0 (1-\sigma_0) = \pi R^2 h (1-\sigma) \tag{2}$$

2.1 Constant speed squeeze

At a given moment, the fluid is squeezed until it reaches the radius R. The flow conservation, in radial coordinates, gives:

$$\pi r^2 V = -\frac{2\pi r \phi h}{\eta} \frac{\mathrm{d}p}{\mathrm{d}r} \tag{3}$$

After separation of variables and simplification, the differential equation of pressure variation is:

$$\frac{\mathrm{d}p}{\mathrm{d}r} = -\frac{\eta V}{2\phi h} r \tag{4}$$

By integration with boundary conditions: $p=0$ at $r=R$, yields:

$$p = \frac{\eta V}{4\phi h}(R^2 - r^2) \tag{5}$$

Integrating equation (5) on disk surface, the expression of force generated by squeeze of porous material with fluid reservoir is:

$$F = \frac{\pi \eta V}{8 \phi h} R^4 \tag{6}$$

In order to determine the dimensionless expression for force, based on the hypothesis (*d*), the compactness σ can be written in terms of the dimensionless thickness $H = h / h_0$.

$$\sigma = \sigma_0 / H \tag{7}$$

From equations (2) and (7), the dimensionless radius $\overline{R} = R / R_0$ can be written as:

$$\overline{R} = \sqrt{\frac{1 - \sigma_0}{H - \sigma_0}} \tag{8}$$

Using the dimensionless notation *H* and equation (7), the Kozeny-Carman equation (1) for the permeability ϕ, can be written as:

$$\phi = \frac{D(H - \sigma_0)^3}{H \sigma_0^{\,2}} \tag{9}$$

Finally, combining equations (6), (8) and (9) we get the dimensionless force as a function of dimensionless thickness, *H*:

$$\overline{F} = \frac{\pi \sigma_0^2 (1 - \sigma_0)^2}{8 (H - \sigma_0)^5} \tag{10}$$

In fig. 2 is presented the variation of dimensionless force written as function of *H,* for different values of HCPL compactness. One can see that the dimensionless force increases with the compactness for a given dimensionless thickness.

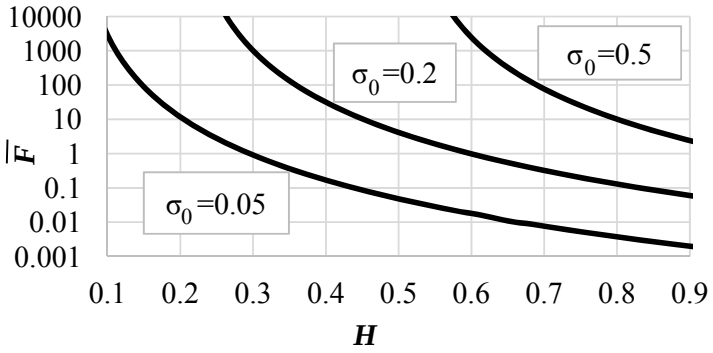

Fig. 2 Dimensionless force $\overline{F}$ vs. dimensionless thickness H

2.2 Constant force squeeze

This model allows determination of squeeze time until a defined thickness (compression level) is obtained. The squeeze speed can be written as:

$$V = -h_0 \mathrm{d}H / \mathrm{d}t \tag{11}$$

If eq. (11) is introduced in eq. (6) and the permeability and thickness are written also dimensionless, yields:

$$-\mathrm{d}\tau = \frac{\pi\sigma_0^2 (1-\sigma_0)^2}{8(H-\sigma_0)^5}\mathrm{d}H, \tag{12}$$

where the dimensionless time τ is defined as $\tau = \dfrac{tFD}{\eta R_0^4}$.

After integration of equation (12) we get:

$$\tau + C = \frac{\pi\sigma_0^2 (1-\sigma_0)^2}{32(H-\sigma_0)^4}\mathrm{d}H \tag{13}$$

Using the initial condition $H = 1$ at $\tau = 0$, the equation for the dimensionless time τ is obtained:

$$\tau = \frac{\pi\sigma_0^2 (1-\sigma_0)^2}{32}\left[\frac{1}{(H-\sigma_0)^4} - \frac{1}{(1-\sigma_0)^4}\right] \tag{14}$$

The variation of the dimensionless thickness H as function of dimensionless time τ is shown in fig. 3. One can see that the time of squeeze increases with the increase of compactness, respectively the decrease of porosity. This is not evident from equation (14), but it is obvious that more time is needed to compress with constant force a material with higher compactness.

When $H = H_{\text{limit}}$, the squeezed fluid reaches the outer margin and $\overline{R} = R_e / R_0$. Further, this theoretical model no longer applies. This limiting thickness, H_{limit}, can be determined as:

$$H_{\text{limit}} = \sigma_0 + \frac{1-\sigma_0}{R_e / R_0} \tag{15}$$

The limit of the squeeze process represented with dashed lines in fig. 3, is obtained when $\overline{R} = 2$. If squeezed below the limit, the fluid flows outside the porous ring until porous material becomes solid.

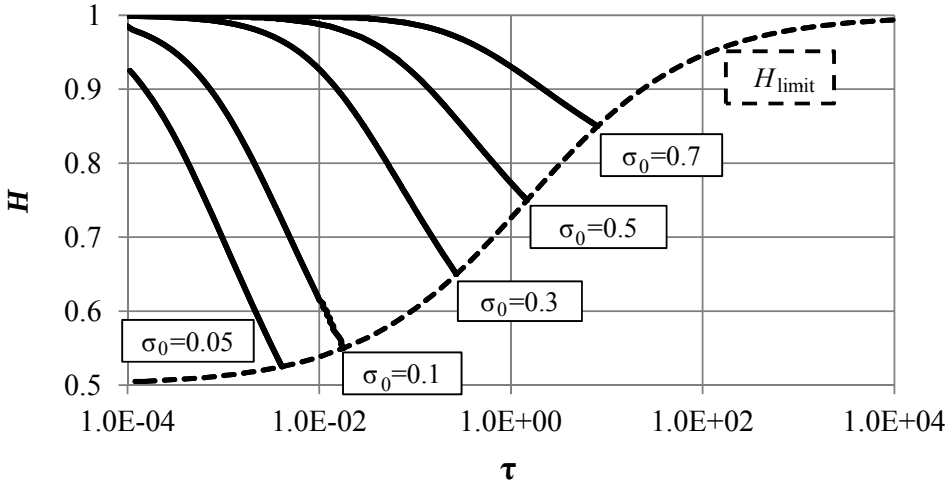

Fig. 3 Variation of dimensionless thickness H vs. dimensionless time τ

2.3 Impact squeeze

Since the impact protection system based on porous ring with reservoir of liquid is a feasible solution, the model was extended for the case of squeeze under impact. The model allows determination of damping capacity for a ring of porous material under impact with a body with known mass *M* and impact speed of V_0. For squeeze under impact the impulse equation is:

$$M\mathrm{d}V = -F \cdot \mathrm{d}t \tag{16}$$

Also, according with Bowden and Tabor model [3], assuming small displacements, it is possible to use the force determined for squeeze with constant speed into eq. (16). Rewriting eq. (10) in dimensional form results:

$$F = -\frac{\pi\eta V R_0^4 \sigma_0^2 (1-\sigma_0)^2}{8D h_0 (H-\sigma_0)^5}\frac{\mathrm{d}h}{\mathrm{d}t} \tag{17}$$

Introducing eq. (17), in eq. (16) and rearranging, results:

$$dV = -\frac{\pi\eta R_0^4 \sigma_0^2 (1-\sigma_0)^2}{8DM}\frac{1}{(H-\sigma_0)^5}dH \tag{18}$$

After integration, yields:

$$V = C + \frac{\pi\eta R_0^4 \sigma_0^2 (1-\sigma_0)^2}{32DM}\frac{1}{(H-\sigma_0)^4} \tag{19}$$

For the initial condition H=1 at t=0, the expression of the speed results:

$$V = V_0 - \frac{\pi\eta R_0^4 \sigma_0^2 (1-\sigma_0)^2}{32DM}\left[\frac{1}{(H-\sigma_0)^4} - \frac{1}{(1-\sigma_0)^4}\right] \tag{20}$$

Finally, introducing eq. (20) in eq. (17) results the force generated during squeeze motion, produced by impact:

$$F = \frac{\pi\eta R_0^4 \sigma_0^2 (1-\sigma_0)^2}{8\, D h_0 (H-\sigma_0)^5} \cdot \left\{V_0 - \frac{\pi\eta R_0^4 \sigma_0^2 (1-\sigma_0)^2}{32DM}\left[\frac{1}{(H-\sigma_0)^4} - \frac{1}{(1-\sigma_0)^4}\right]\right\} \tag{21}$$

Using dimensionless parameters for the force $\overline{F} = FDh_0/(R_0^4\eta)$ and impulse $\overline{M} = MDV_0/(R_0^4\eta)$, eq. (21) becomes:

$$\overline{F} = \frac{\pi\sigma_0^2(1-\sigma_0)^2}{8(H-\sigma_0)^5}\left\{V_0 - \frac{\pi\sigma_0^2(1-\sigma_0)^2}{32\overline{M}}\left[\frac{1}{(H-\sigma_0)^4} - \frac{1}{(1-\sigma_0)^4}\right]\right\}. \tag{22}$$

3. Experimental results

In order to validate the theoretical model a series of experiments at constant speed using UMT-2 CETR universal tribometer were made. The test rig (fig. 4) has two main components: control unit (computer and data acquisition board) and the testing unit (sensor, mobile carriage with indenter, container). The measurement of the force generated during squeeze is made simultaneous with time, displacement and squeeze speed. The precision of carriage vertical displacement is 1 μm and its velocity can be varied between 0.001 -10 *mm/s*. The force sensor DFH-20 mounted on the mobile carriage is capable to measure up to 200 *N* with a resolution of 0.02 *N*. The moving (upper) part is a 66 *mm* diameter steel disc of 5 *mm* thickness.

The experiments were made for rings of porous material with an outer diameter of 66 *mm,* and a central reservoir with diameter of 33 *mm* represented by the same porous material disc imbibed with liquid (see fig. 4). Each disc reservoir was imbibed with fluid prior to each test and placed in the central part of the dry ring.

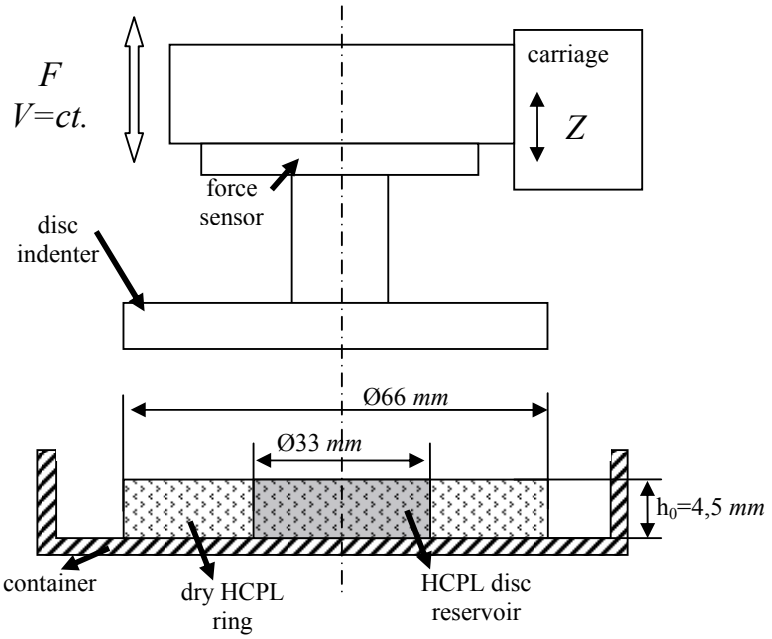

Fig. 4 The experimental test rig

Two fluids were used in experiments: glycerin ($\eta = 0.6\,Pa \cdot s$) and silicone oil ($\eta = 11\ Pa \cdot s$). Glycerin was chosen because its behavior is very similar with a Newtonian fluid. However, it has an important shortcoming when used for damping or protection systems: in the presence of liquid water or vapors the viscosity of glycerin diminishes as a result of its hydrophilic behavior. Silicon oil is considered to be an ideal candidate because of its stability for various conditions of use. However, the non-Newtonian behavior of the silicon oil made it inappropriate for validation of the theoretical model.

The selected porous material is a reticulated polyurethane foam FILTREN® TM 25133 (codification: F133). F133 have an open cellular structure and is usually used as filtering material. Its properties are: density 20-24 kg/m^3 compression resistance 2.5-4.5 *kPa*, ultimate elongation 100%, tensile strength 80 *kPa*. The average pore size varies between 1.06 and 1.6 *mm*. Porosity measurements were carried out and the average value was: $\varepsilon_0 = 0.95$. The initial thickness of the ring as well for the inner reservoir disc radius were h_0=4.5 *mm*. Fig. 5 shows a porous ring of porous material F133 with reservoir of glycerin imbibed before (Fig. 5a) and after squeeze (Fig. 5b) with constant speed. With blue line is marked the limit to which the ring material was imbibed.

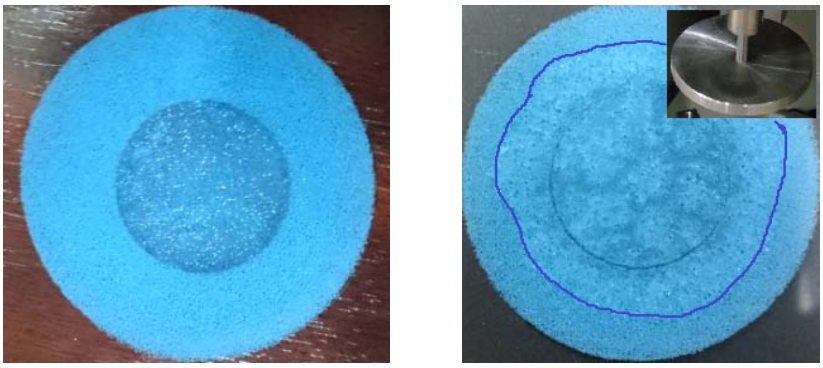

a) b)

Fig. 5 The ring of porous material F133 with reservoir of fluid imbibed *before squeeze* - a) and *after squeeze with constant speed* – b)

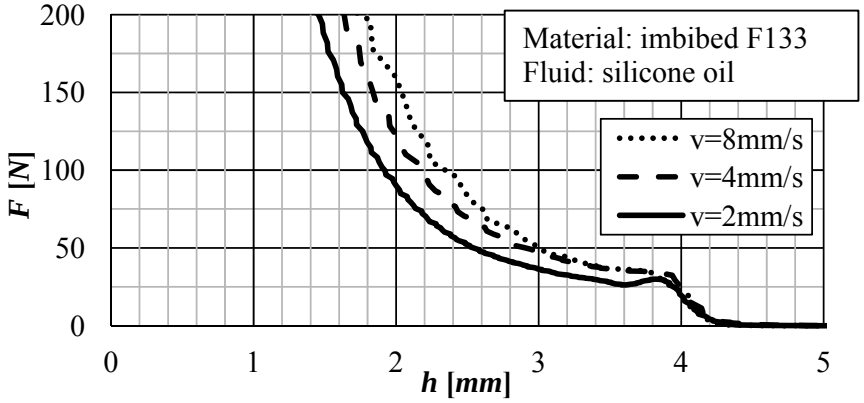

Fig. 6 Squeeze force vs. porous material thickness for reservoir with silicon oil

In fig. 6 and fig. 7 are presented the experimental results with various squeeze speed v = 2, 4 and 8 *mm/s* and a ring reservoir filled with glycerin and silicone oil, respectively. A rapid increase of the force can be observed in the first part of the squeeze motion (for thickness variation between 4.5 *mm* and 3.5 *mm*). This behavior attributed to the solid matrix response to compression. Analyzing further these results, it can be observed that the force increases with the increase of speed from 2 *mm/s* up to 4 *mm/s* and 8 *mm/s*.

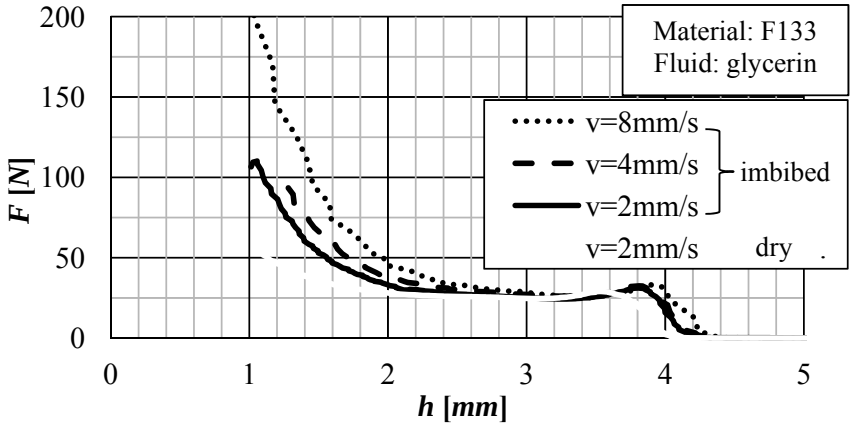

Fig. 7 Force measured on squeeze for reservoir with glycerin

Comparing the forces measured at the same speed (fig. 8), for glycerin and silicone oil it can be seen that the squeeze force is considerably higher for the more viscous fluid (silicone oil).

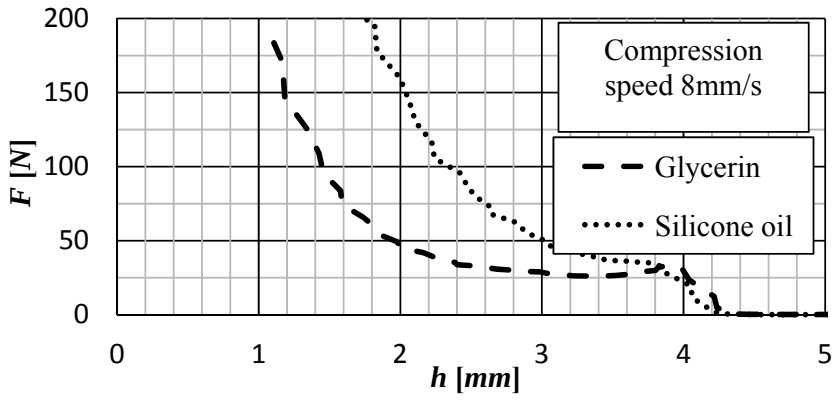

Fig. 8 Comparison between forces measured for squeeze speed v=8 *mm/s*

Despite high performances and good stability characteristics of silicone oil, it is difficult to predict its behavior with present analytical model as a result of its non-Newtonian behavior.

The variation of the force for dry material during squeeze is shown in fig. 7. Even smaller than those measured during squeeze with glycerin, the forces cannot be ignored. Applying the principle of superposition, one can identify the contribution of fluid squeeze only. The resulting force obtained for glycerin, is presented in fig. 9.

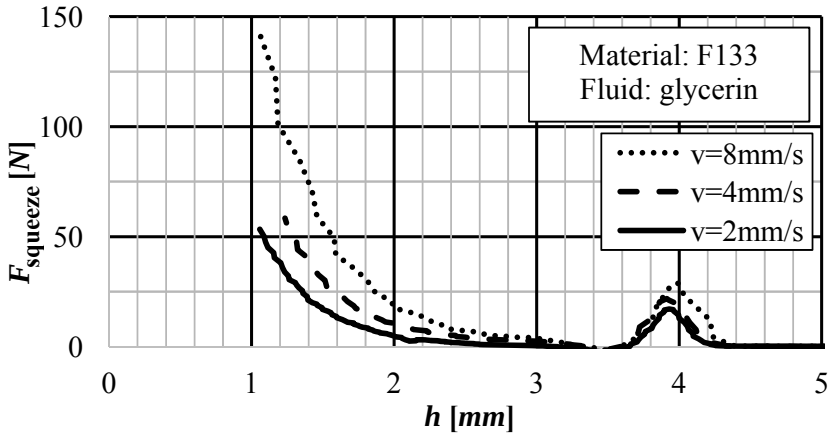

Fig. 9 Fluid squeeze force for glycerin calculated from the experimental data

4. Validation of theoretical model for constant speed squeeze

According to the proposed model, the force generated by constant speed squeeze can be expressed in terms of the instantaneous thickness of the porous layer by replacing equation (9) in equation (6):

$$F = \frac{\pi\eta V(1-\sigma_0)^2 h_0^2 R_0^4 \sigma^2}{8Dh^3\left(1-\frac{\sigma_0 h_0}{h}\right)^5} \tag{23}$$

The values for the parameters used in equation (23) are presented in Table1.

Table 1

Parameter	Value	Parameter	Value
D	$1.3\cdot10^{-10}\ m^2$	R_0	16.5 *mm*
σ_0	0.05	η	0.6 *Pa s*
h_0	4.5 *mm*		

Because no other method was available, for the determination of parameter D, this was calculated using the experimental data and assuming valid the proposed model. Three values of D *(each corresponding to a value of the speed, u*) were calculated by fitting the experimental force with that predicted by the model. The average of these is presented in table 1.

The experimental data for force variation with the layer thickness is compared with the predicted values of the force, calculated with eq. (23) and the results are plotted in fig. 10.

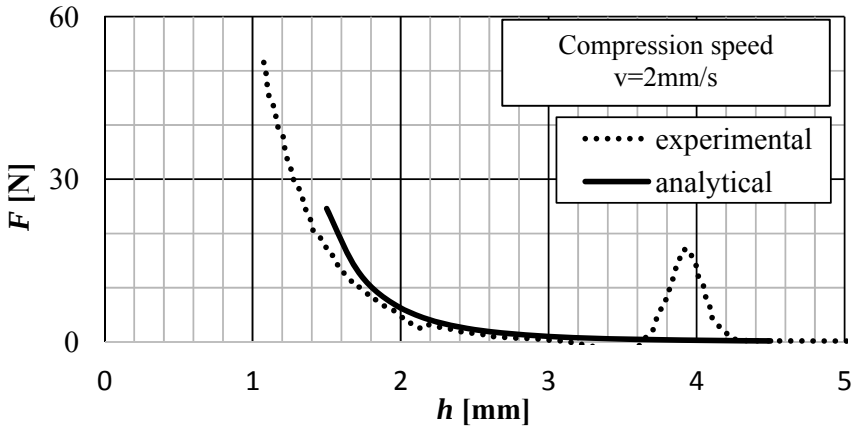

Fig. 10 Experimental vs. analytical results for glycerin at speed 2 *mm/s*

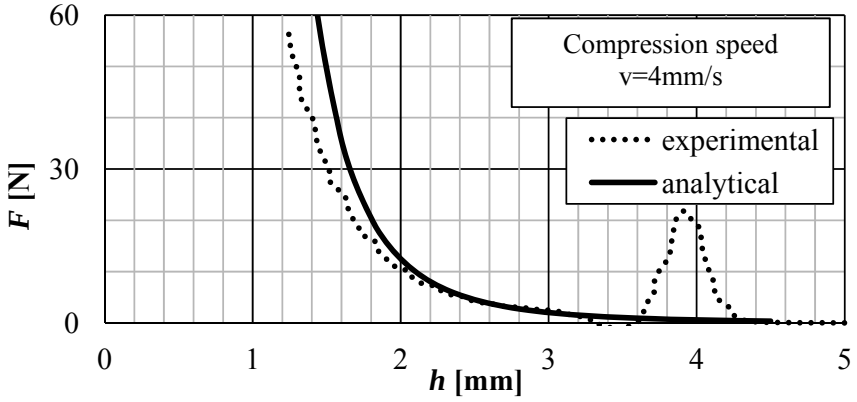

Fig. 11 Experimental vs. analytical results for glycerin at speed 4 *mm/s*

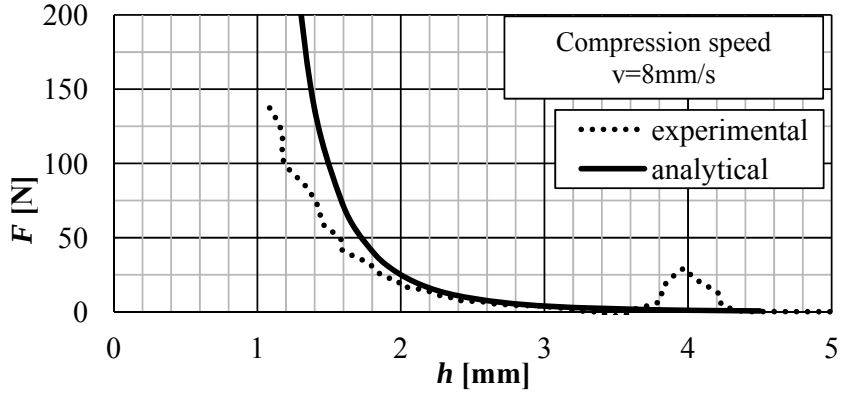

Fig. 12 Experimental vs. analytical results for glycerin at speed 8 *mm/s*

The analytical results are in quite good correlation with the experimental results. It can be concluded that the analytical model is valid. The differences between the experimental data and theoretical results are acceptable. The sources of errors are multiple. The permeability ϕ of the material is defined using Kozeny-Carman equation. The accuracy of this equation is influenced by the parameter *D,* which was obtained by fitting the experimental data for force with the predicted force.

The accuracy of the measured values for the initial layer thickness and material porosity can also be a source of the differences between the values of experimental and analytical force.

A boundary can be found between the imbibed disc reservoir and the annular foam disc. It includes cross-section gaps or blocked pores as result of cutting process.

List of notations

C constant of integration;
D material parameter from Kozeny-Carman equation;
F force; h thickness; M mass; p pressure;
r radial coordinate; R external limit of fluid reservoir;
R_e external radius of the porous ring; t time; V speed.

Indices

0 at initial moment.

Greek alphabet notations

ε porosity;
η dynamic viscosity;
σ compactness;
ϕ permeability.

Dimensionless notations

$\overline{F} = Fh_0 D/(\eta V R_0^4)$ force;
$H = h/h_0$ thickness;
$\overline{R} = R^2/R_0^2$ radius;
$\overline{M} = MDV_0/(R_0^4\eta)$ impulse;
$\tau = tFD/\eta R_0^4$ time.

7. Conclusions

An original theoretical model for a given volume of Newtonian fluid imbibed in central area (reservoir) squeezed through a surrounding porous ring was developed. The theoretical model was developed for three cases of squeeze: with constant speed, constant force and for a given impulse.

The theoretical model was validated using the experimental data for squeeze with constant speed of reticulated polyurethane foam imbibed with glycerin.

The observed differences are mainly related to the fact that the analytical model considers a continuous HCPL without a border between central region (the reservoir) and the dry porous ring. In the experimental model this boundary exists.

Further experiments should be performed for multiple materials and fluids. The influence on performance of the central reservoir dimension must be also evaluated.

Acknowledgements

The work has been supported by Partnerships in Priority Areas Program – PNII implemented with the support of Romanian Ministry of Education – UEFISCDI, project number 287/2014.

R E F E R E N C E S

[1] *M. D. Pascovici*, Lubrication by Dislocation: A New Mechanism for Load Carrying Capacity, Proceedings of 2nd World Tribology Congress, Vienna, 2001, pp.41;

[2] *M. D. Pascovici, T. Cicone*, Squeeze-film of unconformal, compliant and layered contacts, Tribology International, 36, 2003, pp. 791-799;

[3] *M. D. Pascovici, C. S. Popescu, and V. Marian*, Impact of a rigid sphere on a highly compressible porous layer imbibed with a Newtonian liquid, Proc. IMechE Part J: J. Engineering Tribology, Vol. 224, 2010, pp. 789-795;

[4] *M. Radu, T. Cicone,* Experimental determination of the damping capacity of highly compressible porous materials imbibed with water, BALKANTRIB`14, 8th International Conference on Tribology, 2014;

[5] *M. Radu, T. Cicone,* Squeeze effects of an infinitely long, rigid cylinder on a highly compressible porous layer imbibed with liquid, U.P.B. Sci. Bull., Series D, Vol. 76, Iss. 4, 2014

[6] *M.A. Dawson,*. Modeling the dynamic response of low-density, reticulated, elastomeric foam impregnated with Newtonian and Non-Newtonian fluids. PhD Thesis, Massachusetts Institute of Technology; 2008;

[7] *B.G. Vossen*, Modeling the application of fluid filled foam in motorcycle helmets, PhD Thesis, Eindhoven University of Technology; 2010;

[8] *M.D. Pascovici, C. Russu, T. Cicone,* Squeeze film of conformal, layered, compliant and porous contacts, Acta Tehnica Napocensis*,* Series Applied Mathematics and Mechanics, 47, vol.1, 2004;

[9] *M.A. Dowson, G.H. McKinley, L.J. Gibson*, The Dynamic Compressive Response of Open-Cell Foam Impregnated With a Newtonian Fluid, Journal of Applied Mechanics, Vol. 75, 2008;

[10] *M.A. Dowson,* Modeling the dynamic response of low density, reticulated elastomeric foam impregnated with Newtonian and Non-Newtonian fluids, PhD Thesis, Massachusetts Institute of Technology, 2008;

[11] *B.G. Vossen*, Modeling the application of fluid filled foam in motorcycle helmets, PhD Thesis, Eindhoven University of Technology; 2010;

[12] *M.A. Dawson, J.T. Germaine, L.J. Gibson*, Permeability of open-cell foams under compressive strain, Journal of Solids and Structures 44, 2007, pp: 5133-5145;

[13] *G. Pampolini,* Les proprietes mecaniques des mousses polymeriques a cellules ouvertes: experiences, modele theorique et simulations numeriques, PhD thesis, University of Provence France and University of Ferrara Italy, 2010;

[14] *Scheidegger A. E.,* The physics of flow through porous media, 3rd edition, 1974, University of Toronto Press, Toronto and Buffalo.

[15] *H. Darcy*, Les fontaines publiques de la ville de Dijon, Paris: Dalmont, 1856;

[16] *Feng J.***,** *Weinbaum, S.***,** Lubrication theory in highly compressible porous media: the mechanics of skiing, from red cells to humans. *J. Fluid Mech.*, 2000, 422, 281–317.